

A Variational Multiscale Method to Embed Micromechanical Surface Laws in the Macromechanical Continuum Formulation

K. Garikipati¹

Abstract: The embedding of micromechanical models in the macromechanical formulation of continuum solid mechanics can be treated by a variational multiscale method. A scale separation is introduced on the displacement field into coarse and fine scale components. The fine scale displacement is governed by the desired micromechanical model. Working within the variational framework, the fine scale displacement field is eliminated by expressing it in terms of the coarse scale displacement and the remaining fields in the problem. The resulting macromechanical formulation is posed solely in terms of the coarse scale displacements, but is influenced by the fine scale; thereby it has a multiscale character. The procedure results in an embedding of the micromechanical model in the macromechanical formulation. In this paper, this general approach is presented for the special case of traction-displacement laws on internal surfaces. Numerical examples are presented that demonstrate the method for several benchmark problems.

keyword: Multiscale deformation, variational methods, surface laws, embedding, micromechanics.

1 Introduction

Surface laws manifest themselves in a number of ways within the context of macromechanical continuum solid mechanics. Some examples are: (i) the evolution of shear stress driven by tangential slip on an internal surface, (ii) the decay of normal traction with opening of a fracture surface, (iii) the evolution of traction driven by slip and normal separation on a fracture surface and (iv) the variation of traction across the contact surface between two bodies as a function of relative motion of the surfaces. Given appropriate macromechanical, phenomenological, continuum models, a family of traction-displacement laws can be obtained that fit the description

of (i)—(iii) above. The analysis of phenomenological models of plasticity and damage that admit discontinuous solutions yields such laws [Simo, Oliver, Armero (1993); Simo, Oliver (1994); Armero, Garikipati (1995); Larson, Runesson, Akesson (1995); Armero, Garikipati (1996); Oliver (1996); Svedberg, Runesson (1998); Armero, Callari (1999); Regueiro, Borja (1999)]. Adopting a distributional viewpoint, the strain has a singular character (a Dirac delta function); however, careful arguments reveal that the inelastic constitutive models remain well-defined. The location of the discontinuity, specified by a one-dimensional Heaviside function, defines the internal surface. The distributional analysis reveals that the traction on this surface evolves with the normal and tangential components of displacement across the surface, usually in a decaying fashion.

In a contrasting scenario a bifurcation could provide the conditions from which further evolution is governed by a chosen traction-displacement law [Rice (1976)]. Such an approach and the method described in the preceding paragraph are commonly employed to model the localization of deformation. For contact problems, nonlinear and nonlocal traction-displacement laws can be formulated that take account of the micromechanics of interlocking and deforming asperities [Oden, Pires (1983)]. The cases of interest in this paper correspond to examples (i)—(iii) in the previous paragraph. It is desired to treat micromechanical surface laws that are specified independently of the macromechanical formulation. These laws could arise from considerations that fall beyond the scope of the macromechanical formulation. They might even be specified on an empirical basis, drawing from experiments. In this sense, an embedding of the micromechanical surface laws is sought within the macromechanical continuum formulation.

To the knowledge of the author, a statement of the problem in these terms has not appeared previously in the literature. Several approaches might be possible to effect

¹ Department of Mechanical Engineering, University of Michigan, Ann Arbor, MI 48109

such embeddings. The approach to be pursued here is called the Variational Multiscale Method. It has been applied earlier to theoretical and computational aspects of problems of localized deformation [Garikipati, Hughes (1998); Garikipati, Hughes (2000a)]. In subsequent work, the idea of embedding micromechanical surface laws was broached and presented in a one-dimensional setting that allowed a closed-form solution [Garikipati, Hughes (2000b)]. The present paper can be viewed as an extension of that work to multiple dimensions and the macromechanical setting of finite strain plasticity.

The underlying principles to embedding micromechanical laws via the variational multiscale method are elementary. A scale separation is introduced on the displacement field into coarse and fine scale components. Correspondingly, two systems of equations are identified: the macromechanical continuum formulation and the micromechanical surface law. Using the latter, the fine scale displacement is expressed as a functional of the coarse scale displacement and the remaining fields. Finally, this functional is substituted for the fine scale in the standard weak form of the macromechanical problem. The fine scale displacement does not appear explicitly in the resulting weak form; however, this weak form is modified by the above procedure. It can be regarded as having the fine scales projected on to the coarse scales. The use of the micromechanical surface law also results in it being embedded within the multiscale, macromechanical formulation.

A related but different problem is the application of homogenization theory to calculate the effective material properties and multiscale solution field in a material with regularly dispersed inhomogeneities. While multiscale fields arise due to the microstructure, the constitutive assumption remains that of linear elasticity. See References [Fish, Belsky (1995a); Fish, Belsky(1995b); Zohdi, Oden, Rodin (1996); Oden, Zohdi (1997); Moes, Oden, Kumar, Rémacle (1999); Oden, Kumar, Moes (1999)] for recent examples of such methods. The distinguishing aspect of the class of problems being considered here is that the micromechanical aspects are represented by a separate set of constitutive relations and balance laws. Furthermore, the macromechanical continuum description is applicable almost everywhere; it is only over a finite number of subdomains that the micromechanical description prevails.

Details of the formulation are worked out in Section 2,

and numerical examples are presented in Section 3. Section 4 provides a summary and also indicates additional areas where these methods can be applied.

2 The variational multiscale formulation

The weak form of the problem is the point-of-departure for the developments. Since the macromechanical continuum setting is that of *isochoric*, multiplicative finite strain plasticity, appropriate mixed variational formulations must be used to treat numerical issues arising out of the incompressibility constraint [Garikipati, Hughes (2000a)]. The weak form, (W) , is obtained as the Euler-Lagrange equations of a three-field Hu-Washizu variational principle, wherein the independent unknowns are the displacement, \mathbf{u} , the scalar field, Θ , representing the local ratio of current to initial volumes and, a second scalar, p , representing the hydrostatic Kirchhoff stress [Simo, Taylor, Pister (1985)].

$$\begin{aligned}
 \int_{\Omega} (\text{dev}[\nabla \mathbf{w}] : \boldsymbol{\tau} + \text{div}[\mathbf{w}]p) dV &= \int_{\Omega} \mathbf{w} \cdot \mathbf{f} dV \\
 &+ \int_{\partial\Omega_t} \mathbf{w} \cdot \mathbf{T} dS \\
 \int_{\Omega} \frac{q}{\Theta} (J - \Theta) dV &= 0 \\
 \int_{\Omega} \gamma \frac{(-p + \frac{1}{3}\text{tr}[\boldsymbol{\tau}])}{\Theta} dV &= 0 \quad (1)
 \end{aligned}$$

The first line in Equation (1) is a weak statement of balance of linear momentum, where \mathbf{w} is the displacement weighting function—also referred to as the variation on the displacement, $\boldsymbol{\tau}$ is the Kirchhoff stress, \mathbf{f} is the body force and \mathbf{T} is the traction. The second line is a weak imposition of the requirement that the scalar, Θ , be equal to the jacobian of the deformation, J . Here, q is the variation corresponding to the hydrostatic stress field, p . Finally, the third line weakly enforces the relation between p and the hydrostatic Kirchhoff stress, $\boldsymbol{\tau}$, where γ is the variation corresponding to Θ . The symbol $\text{tr}[\bullet]$ represents the trace of a tensor argument, $\text{dev}[\bullet]$ is the deviatoric component and $\text{div}[\bullet]$ is the divergence.

A scale separation is now introduced by a decomposition of the displacement, \mathbf{u} , into coarse scale component, $\bar{\mathbf{u}}$, and fine scale component, \mathbf{u}' . Such a decomposition is also imposed upon the displacement weighting function,

\mathbf{w} . The decomposition is made precise by requiring that the fine scales, \mathbf{u}' and \mathbf{w}' , vanish outside of some region Ω' , which will be referred to as the microstructural or fine scale subdomain.

$$\begin{aligned} \mathbf{u} &= \underbrace{\bar{\mathbf{u}}}_{\text{coarse scale}} + \underbrace{\mathbf{u}'}_{\text{fine scale}}, \\ \mathbf{w} &= \underbrace{\bar{\mathbf{w}}}_{\text{coarse scale}} + \underbrace{\mathbf{w}'}_{\text{fine scale}} \\ \mathbf{u}', \mathbf{w}' &\in \mathcal{S}' = \{\mathbf{v}' | \mathbf{v}' = 0 \text{ on } \Omega \setminus \text{int}(\Omega')\} \end{aligned} \quad (2)$$

Given the decomposition in Equation (2), the weak form, Equation (1), can be split into two separate weak forms. One, involving coarse scale weighting function, $\bar{\mathbf{w}}$, is termed the Weak Form of the Coarse Scale Problem, (\bar{W}) , and the other, involving only fine scale weighting functions, \mathbf{w}' , is termed the Weak Form of the Fine Scale Problem, (W') .

$$\begin{aligned} \int_{\Omega} (\text{dev}[\nabla \bar{\mathbf{w}}] : \boldsymbol{\tau} + \text{div}[\bar{\mathbf{w}}]p) dV &= \int_{\Omega} \bar{\mathbf{w}} \cdot \mathbf{f} dV \\ (\bar{W}) &+ \int_{\partial\Omega_i} \bar{\mathbf{w}} \cdot \mathbf{T} dS \\ \int_{\Omega} \frac{q}{\Theta} (J - \Theta) dV &= 0 \\ \int_{\Omega} \gamma \frac{(-p + \frac{1}{3}\text{tr}[\boldsymbol{\tau}])}{\Theta} dV &= 0, \end{aligned} \quad (3)$$

$$\begin{aligned} \int_{\Omega'} (\text{dev}[\nabla \mathbf{w}'] : \boldsymbol{\tau} + \text{div}[\mathbf{w}']p) dV &= \int_{\Omega'} \mathbf{w}' \cdot \mathbf{f} dV \\ (W') &+ \int_{\partial\Omega'_i} \mathbf{w}' \cdot \mathbf{T} dS. \end{aligned} \quad (4)$$

Importantly, this procedure results in the weak form of the fine scale problem, (W') , being defined only over Ω' . This result is crucial since it lends itself naturally to the application of desired micromechanical descriptions restricted to the microstructural region, Ω' . For a particular choice of micromechanical law, the fine scale solution, \mathbf{u}' , is to be expressed in terms of $\bar{\mathbf{u}}$ and other fields in the problem via the fine scale weak form, (W') . The final step involves elimination of the fine scale, \mathbf{u}' , from the problem by substituting such an expression in the coarse scale

weak form, (\bar{W}) . Thus the fine scale solution does not appear explicitly; however, its effect is fully embedded in the resulting modified weak form, termed the Weak Form of the Multiscale Method, (\bar{W}) . In principle, the step of expressing \mathbf{u}' in terms of the coarse scale, $\bar{\mathbf{u}}$, and the remaining fields may be carried out either exactly or approximately. In virtually any case of practical interest, the exact solution is intractable. Of the available approximate methods, the chosen representation may be either analytic or numerical.

2.1 The micromechanical surface law

Having established the above general setting, a surface, $\Gamma \subset \Omega'$ (Figure 1), is introduced. The micromechanical law is to be specified on Γ . In the present finite strain setting, the surface Γ can be viewed in either the reference or spatial configuration as in Figure 1.

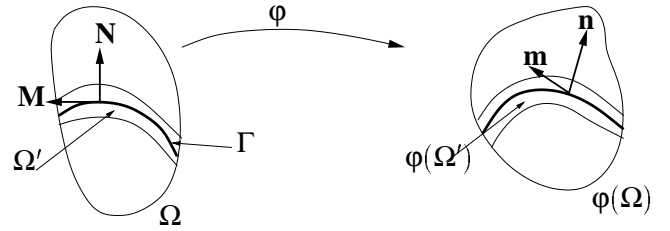


Figure 1 : Surface Γ , its normal \mathbf{N} and tangent \mathbf{M} in the reference configuration, Ω , mapped forward by the deformation ϕ to spatial configuration $\phi(\Omega)$.

Invoking standard variational arguments, the weak form of the fine scale problem can be reduced to the following statement of traction continuity:

$$[[\boldsymbol{\tau}\mathbf{n}]]_{\Gamma} = 0, \quad \mathbf{n} = \mathbf{F}^{-T}\mathbf{N}, \quad (5)$$

where $\boldsymbol{\tau}\mathbf{n}$ is the traction vector and \mathbf{n} is the pushed forward normal (Figure 1). Writing the traction on Γ in terms of components T_n and T_m along \mathbf{n} and \mathbf{m} respectively (Figure 1), the traction continuity equation (5) can be cast into the form

$$T_n\mathbf{n} + T_m\mathbf{m} = \boldsymbol{\tau}\mathbf{n}|_{\Gamma^-}, \quad (6)$$

where $\mathbf{n} = \mathbf{F}^{-T}\mathbf{N}$ and $\mathbf{m} = \mathbf{F}^{-T}\mathbf{M}$.

The traction, $\boldsymbol{\tau}\mathbf{n}|_{\Gamma^-}$, is determined by the macromechanical continuum formulation. The evolution of traction

components on Γ is governed by the micromechanical surface law. It is desired to allow a discontinuous displacement $[[\mathbf{u}]]$, and to express it in terms of the normal opening, ξ_n , and tangential slip, ξ_m , across Γ .

$$[[\mathbf{u}]] = \mathbf{F} \begin{pmatrix} \underbrace{\xi_n \mathbf{N}}_{\text{Mode 1}} + \underbrace{\xi_m \mathbf{M}}_{\text{Mode 2}} \end{pmatrix} \quad (7)$$

Observe that this allows a mixed mode evolution of the displacement jump $[[\mathbf{u}]]$ on Γ . Assuming tensile normal traction, $T_n \geq 0$, and positive tangential traction, $T_m \geq 0$, they are driven by displacement components $\xi_n > 0$ and $\xi_m > 0$, respectively, via the simple micromechanical laws:

$$T_n = T_{n_0} - H_n \xi_n, \quad T_m = T_{m_0} - H_m \xi_m, \quad (8)$$

where $T_{n_0} > 0$ and $T_{m_0} > 0$ are the maximum values of T_n and T_m respectively and $H_n > 0, H_m > 0$ model softening response. Consistency between the micromechanical law and the macromechanical continuum description is enforced by Equation (6) via Equation (8).

2.2 A specific multiscale decomposition

Attention is now turned to embedding the micromechanical law. This involves the explicit definition of coarse and fine scale fields. With the introduction of a discontinuous displacement on the surface Γ , the deformation field is written as

$$\varphi(\mathbf{X}) = \underbrace{\mathbf{X}}_{\text{continuous}} + \underbrace{\hat{\mathbf{u}}(\mathbf{X})}_{\text{discontinuous}} + \underbrace{\mathbf{F}(\xi_m \mathbf{M} + \xi_n \mathbf{N})}_{\text{discontinuous} \cdot [[\mathbf{u}]]} \cdot H_\Gamma \quad (9)$$

The Heaviside function, H_Γ , acts to enforce the discontinuous nature of the displacement jump, $[[\mathbf{u}]]$. Turning to the one-dimensional setting of Figure 2 for motivation, it is observed that for a displacement field admitting a discontinuity, a coarse scale approximation, $\bar{\mathbf{u}}$, can be constructed via the interpolation $\bar{N}(\mathbf{X})$, depicted as a broken line. The difference between the actual field and $\bar{\mathbf{u}}$ appears in the center of the figure. Such a field can be approximated via the interpolation $N'(\mathbf{X})$ on the right.

In a discrete setting, the coarse and fine scale fields are obtained via the interpolations

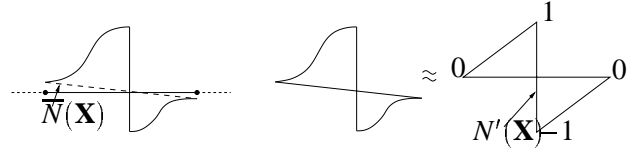


Figure 2 : Coarse and fine scale interpolations $\bar{N}(\mathbf{X})$ and $N'(\mathbf{X})$ in a one-dimensional setting.

$$\begin{aligned} \bar{\mathbf{u}}^h(\mathbf{X}) &= \sum_{A=1}^{n_{\text{node}}} \mathbf{d}^A \bar{N}_A(\mathbf{X}), \\ \mathbf{u}^h(\mathbf{X}) &= \mathbf{F}^h \underbrace{(\xi_m \mathbf{M} + \xi_n \mathbf{N})}_{[[\mathbf{u}]]} N'(\mathbf{X}), \end{aligned} \quad (10)$$

where \mathbf{d}^A are nodal values of $\bar{\mathbf{u}}^h$, n_{node} is the number of nodes in a finite element discretization, and, as is the convention, superscript $(\bullet)^h$ denotes a finite-dimensional approximation to the corresponding field.

Such an additive decomposition of the displacement leads to a multiplicative decomposition of the deformation gradient as

$$\mathbf{F}^h = \underbrace{\left(\mathbf{1} + \sum_{A=1}^{n_{\text{node}}} \mathbf{d}^A \otimes \frac{\partial \bar{N}}{\partial \mathbf{X}} \right)}_{\bar{\mathbf{F}}^h} \underbrace{\left(\mathbf{1} - (\xi_m \mathbf{M} + \xi_n \mathbf{N}) \otimes \frac{\partial N'}{\partial \mathbf{X}} \right)^{-1}}_{\mathbf{F}^h}. \quad (11)$$

In Equation (11), $\bar{\mathbf{F}}^h$ and \mathbf{F}^h are respectively the coarse scale and fine scale deformation gradients.

With this elucidation of multiscale kinematics, we return to the embedding: Equation (6) enforces consistency between the micromechanical and macromechanical descriptions. Taken together with Equation (8) it relates the discontinuous displacement components ξ_n and ξ_m to the macromechanical fields in $\Omega \setminus \Gamma$. Since ξ_n and ξ_m determine the fine scale through Equation (10), it follows that Equations (6), (8) and (10), taken together, express the fine scale field, \mathbf{u}' , in terms of the macromechanical fields. To demonstrate this we proceed as follows:

Defining $\mathbf{m}^\sharp := \mathbf{F}\mathbf{M}$, and $\mathbf{n}^\sharp := \mathbf{F}\mathbf{N}$, Equation (10) gives

$$\mathbf{u}^h = [[\mathbf{u}]]^h N' = (\xi_m \mathbf{m}^\sharp + \xi_n \mathbf{n}^\sharp) N', \quad (12)$$

from which, $\xi_m = [[\mathbf{u}]] \cdot \mathbf{m}$, and $\xi_n = [[\mathbf{u}]] \cdot \mathbf{n}$. Using these

relations and Equation (8) in (6) gives

$$(T_{n_0} - H_n(\llbracket \mathbf{u} \rrbracket \cdot \mathbf{n})) \mathbf{n} + (T_{m_0} - H_m(\llbracket \mathbf{u} \rrbracket \cdot \mathbf{m})) \mathbf{m} - \boldsymbol{\tau} \mathbf{n} = 0, \quad (13)$$

where the last term on the left hand-side is to be evaluated at Γ^- as in Equation (6). The aim is to use Equation (13) to solve for \mathbf{u}' . However, this is a nonlinear relation in \mathbf{u}' since $\boldsymbol{\tau} = (\partial\psi/\partial\mathbf{F}^e)\mathbf{F}^{eT}$, where ψ is the strain energy function, \mathbf{F}^e and \mathbf{F}^p are the elastic and plastic deformation gradients respectively and $\mathbf{F} = \mathbf{F}^e\mathbf{F}^p = \bar{\mathbf{F}}\mathbf{F}'$. Since closed-form solutions for \mathbf{u}' are, in general, difficult to come by, Equation (13) is expanded up to first order terms, denoted $\delta(\bullet)$:

$$\begin{aligned} & (T_{n_0} - H_n(\llbracket \mathbf{u} \rrbracket \cdot \mathbf{n})) \mathbf{n} + (T_{m_0} - H_m(\llbracket \mathbf{u} \rrbracket \cdot \mathbf{m})) \mathbf{m} - \boldsymbol{\tau} \mathbf{n} \\ & - H_n(\delta\llbracket \mathbf{u} \rrbracket \cdot \mathbf{n}) \mathbf{n} + H_n(\llbracket \mathbf{u} \rrbracket \cdot (\nabla\delta\bar{\mathbf{u}} + \nabla\delta\mathbf{u}')^T) \mathbf{n} \\ & - (T_{n_0} - H_n(\llbracket \mathbf{u} \rrbracket \cdot \mathbf{n})) (\nabla\delta\bar{\mathbf{u}} + \nabla\delta\mathbf{u}')^T \mathbf{n} \\ & - H_m(\delta\llbracket \mathbf{u} \rrbracket \cdot \mathbf{m}) \mathbf{m} + H_m(\llbracket \mathbf{u} \rrbracket \cdot (\nabla\delta\bar{\mathbf{u}} + \nabla\delta\mathbf{u}')^T) \mathbf{m} \\ & - (T_{m_0} - H_m(\llbracket \mathbf{u} \rrbracket \cdot \mathbf{m})) (\nabla\delta\bar{\mathbf{u}} + \nabla\delta\mathbf{u}')^T \mathbf{m} \\ & - (\mathbf{C}^{\text{ep}} : (\nabla\delta\bar{\mathbf{u}} + \nabla\delta\mathbf{u}')) \mathbf{n} + (\nabla\delta\bar{\mathbf{u}} + \nabla\delta\mathbf{u}') \boldsymbol{\tau} \mathbf{n} = 0, \end{aligned} \quad (14)$$

where the first line in (14) represents a zeroth-order approximation to (13), and the remaining terms are the first-order corrections. The elastoplastic tangent in the spatial configuration is written as \mathbf{C}^{ep} . Using $\mathbf{u}' = \llbracket \mathbf{u} \rrbracket N'$ renders this a linear equation in $\delta\llbracket \mathbf{u} \rrbracket$ which can be solved, and the incremental fine scale field constructed as $\delta\mathbf{u}' = \delta\llbracket \mathbf{u} \rrbracket N'$. Formally, it is represented as,

$$\delta\mathbf{u}' = U' [\bar{\mathbf{u}}, \boldsymbol{\tau}, \mathbf{f}, \mathbf{t}, T_m, T_n, \xi_m, \xi_n]. \quad (15)$$

The weak form of the coarse scale problem, Equation (3), involves the jacobian of the deformation, $J = \det[\bar{\mathbf{F}}\mathbf{F}']$, and the scalar field, Θ , which is weakly related to J . Recall that under the elastoplastic multiplicative decomposition, $\mathbf{F} = \mathbf{F}^e\mathbf{F}^p$, the Kirchhoff stress is $\boldsymbol{\tau} = (\partial\psi/\partial\mathbf{F}^e)\mathbf{F}^{eT}$, where ψ , \mathbf{F}^e and \mathbf{F}^p were introduced following Equation (13). Furthermore, the scalar, p , is weakly related to $\text{tr}[\boldsymbol{\tau}]$. From Equations (11) and (10) it then follows that (\bar{W}) depends nonlinearly upon the fine scale displacement, \mathbf{u}' . As with the fine scale solution, this difficulty is surmounted by expanding (\bar{W}) up to terms of first-order in $\nabla\delta\bar{\mathbf{u}}$ and $\nabla\delta\mathbf{u}'$:

$$\begin{aligned} & \int_{\Omega} (\text{dev}[\nabla\bar{\mathbf{w}}] : \boldsymbol{\tau} + \text{div}[\bar{\mathbf{w}}]p) dV \\ & + \int_{\Omega} (\text{dev}[\nabla\bar{\mathbf{w}}] : (\nabla\delta\bar{\mathbf{u}} + \nabla\delta\mathbf{u}') \boldsymbol{\tau}) dV \\ & + \int_{\Omega} \left(\text{div}[\bar{\mathbf{w}}] \frac{1}{3} \text{tr}[\nabla\delta\bar{\mathbf{u}} + \nabla\delta\mathbf{u}'] p \right) dV \\ & + \int_{\Omega} \text{dev}[\nabla\bar{\mathbf{w}}] : \mathbf{C}^{\text{ep}} : (\nabla\delta\bar{\mathbf{u}} + \nabla\delta\mathbf{u}') dV \\ & = \int_{\Omega} \bar{\mathbf{w}} \cdot \mathbf{f} dV + \int_{\partial\Omega_t} \bar{\mathbf{w}} \cdot \mathbf{T} dS, \\ & \int_{\Omega} \frac{q}{\Theta} (J - \Theta) dV + \int_{\Omega} \frac{q}{\Theta} J \text{div}[\delta\bar{\mathbf{u}} + \delta\mathbf{u}'] dV = 0, \\ & \int_{\Omega} \gamma \frac{(-p + \frac{1}{3} \text{tr}[\boldsymbol{\tau}])}{\Theta} dV \\ & + \int_{\Omega} \frac{\gamma}{\Theta} \frac{1}{3} \text{tr}[\mathbf{C}^{\text{ep}} : (\nabla\delta\bar{\mathbf{u}} + \nabla\delta\mathbf{u}')] dV \\ & + \int_{\Omega} \frac{\gamma}{\Theta} \frac{1}{3} \text{tr}[(\nabla\delta\bar{\mathbf{u}} + \nabla\delta\mathbf{u}') \boldsymbol{\tau} + \boldsymbol{\tau} (\nabla\delta\bar{\mathbf{u}} + \nabla\delta\mathbf{u}')^T] dV = 0, \end{aligned} \quad (16)$$

and substituting the fine scale equation, (15), for $\delta\mathbf{u}'$. The fine scale field, $\delta\mathbf{u}'$, is thus eliminated and the weak form of the coarse scale problem is modified to yield the Weak Form of the Multiscale Method, (\bar{W}), which is now posed in terms of $\delta\bar{\mathbf{u}}$. However, the influence of the fine scale field is not lost, but is retained through U' . On solving for $\delta\bar{\mathbf{u}}$, the incremental fine scale field, $\delta\mathbf{u}'$ can be recovered via Equation (15). Iterations are to be performed: $\bar{\mathbf{u}}^{(i+1)} = \bar{\mathbf{u}}^{(i)} + \delta\bar{\mathbf{u}}$, $\mathbf{u}^{(i+1)} = \mathbf{u}^{(i)} + \delta\mathbf{u}'$, until a converged solution is obtained.

From Equations (14) and (15) it should be clear that this procedure also results in an embedding of the micromechanical surface law in the Weak form of the Multiscale Method.

It is noted that the use of the superscript $(\bullet)^h$ has been dispensed with in Equations (13)–(16) for the sake of clarity. The subscript is, however, implied for all fields obtained from the discretized displacements, $\bar{\mathbf{u}}^h$ and \mathbf{u}'^h .

Remark 1: The introduction of a fine scale displacement, \mathbf{u}' might raise the question of whether there is implied a “fine scale force or stress”. No such implication is intended here. Instead there are micromechanical surface stresses, T_m and T_n arising from the chosen law in Equations (6) and (8).

Remark 2: A straightforward analysis reveals that the

resulting system of linearized equations, (14) and (16) is nonsymmetric.

3 Numerical examples

This section briefly discusses three numerical examples demonstrating the embedding of the micromechanical law. The stored energy function is quadratic in logarithmic principal elastic stretches:

$$\begin{aligned}\psi &= \hat{\psi}(J^e, \bar{\lambda}_1^e, \bar{\lambda}_2^e, \bar{\lambda}_3^e) \\ &= \frac{1}{2} \kappa [\log J^e]^2 \\ &\quad + \mu \left[(\log \bar{\lambda}_1^e)^2 + (\log \bar{\lambda}_2^e)^2 + (\log \bar{\lambda}_3^e)^2 \right], \\ J^e &= \det[\mathbf{F}^e], \\ \log \bar{\lambda}_i^e &= \log \lambda_i^e - \frac{1}{3} \log(\lambda_1^e \lambda_2^e \lambda_3^e),\end{aligned}\quad (17)$$

where $\lambda_i^e, i = 1 \dots 3$ are the principal elastic stretches. The bulk and shear modulus are $\kappa = 164.206$ GPa and $\mu = 80.1938$ GPa respectively. The material is also assumed to have an elastic-perfectly plastic response with a yield stress, $\sigma_Y = 450$ MPa. The internal surface, Γ , is assumed to form at any point in the material when the local spatial tangent modulus tensor loses strong ellipticity. This condition is commonly encountered in strain localization problems with softening plasticity or damage, and with nonassociative flow rules [Rice(1976); Willam(1984); Ottosen and Runesson(1991); Armero and Garikipati(1996)]. The traction components, T_m and T_n then begin to evolve along Γ according to Equation (8). For the micromechanical law, T_{m_0} and T_{n_0} are taken as the tangential and normal traction components along Γ at the instant when strong ellipticity is lost. The softening moduli, H_m and H_n , are each taken equal to 0.6667 GPa. The examples assume plane strain conditions.

3.1 Shear along a plane

The first example is one of simple shear in a slab (Figure 3).



Figure 3 : Schematic representation of micromechanical law on a plane parallel to shearing displacement.

When the loss of strong ellipticity is observed in the macromechanical material model, the micromechanical surface, Γ , forms as depicted in Figure 3. The embedded micromechanical law becomes active. In this case it reduces to the tangential component of traction driven by the slip on Γ . Figure 4 shows the undeformed and deformed meshes. The shaded region is the microstructural subdomain (containing Γ) where the fine scale decomposition holds. Observe the sharply resolved deformation around the micromechanical surface. This is despite the fact that the mesh is coarse and completely unstructured.

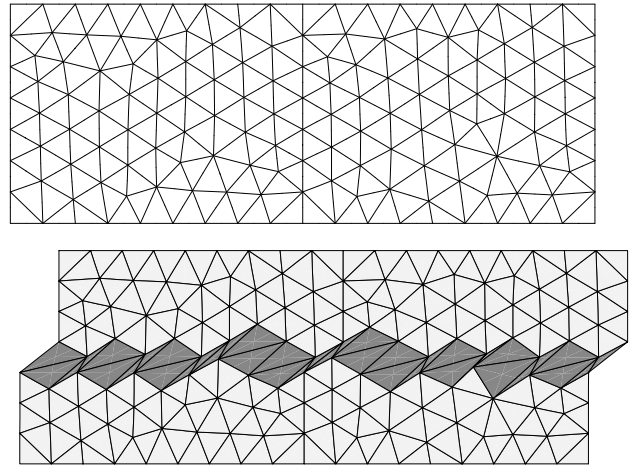


Figure 4 : Deformed mesh and shaded microstructural region for the simple shear problem.

A well-known pathology that is observed with softening continuum material models is the strong dependence of the global load-displacement response upon the mesh size [Bazant (1976)]. Specifically, the softening portion of the curve displays an increasingly negative slope as the mesh is made finer, and this slope does not converge to a limit. Physically, this arises as the size of the region over which thermodynamic dissipation is observed tends to zero with the element size. It is related to an ill-posedness of softening continuum material models. However, the incorporation of traction-displacement laws regularizes the problem [Garkipati and Hughes(1998)]. This important property is retained when such laws are embedded by the variational multiscale method as demonstrated by Figure 5.

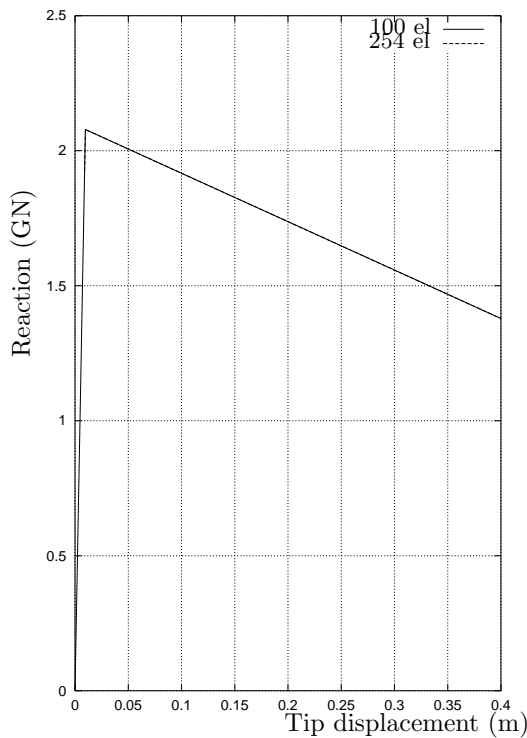


Figure 5 : Load-displacement curves for two uniform meshes with different element sizes. Observe that mesh size-dependent pathologies are absent.

3.2 Inclined plane under tension

The case of the micromechanical law specified along an inclined plane in a bar subjected to tension is considered next (Figure 6).



Figure 6 : Schematic representation of micromechanical law on a plane, Γ , inclined to applied tensile loading.

The activation of the micromechanical law is based on the strong ellipticity condition as described above. Figure 7 shows the undeformed and deformed meshes. Attention is again drawn to the sharp resolution of deformation around the microstructural region (shaded) which encloses the surface Γ of Figure 6.

As with the shear problem, the numerical results obtained are devoid of mesh size-dependent pathology (plots not shown here); i.e., the thermodynamic dissipation is inde-

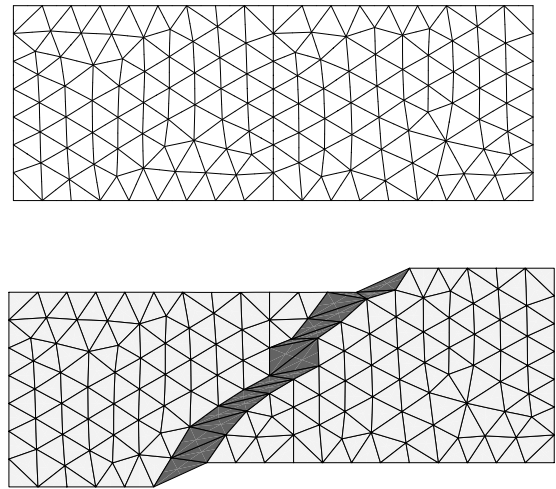


Figure 7 : Deformed mesh and shaded microstructural region for the tension problem.

pendent of mesh size.

3.3 Slipline in a wedge

For this third example the micromechanical law is specified on a slipline in a wedge (Figure 8). The surface forms and extends when the loss of strong ellipticity is satisfied at each point in the wedge in response to the penetrating block. The material parameters are modified to $\kappa = 16.667\text{GPa}$, $\mu = 7.6923\text{GPa}$, $H_m, H_n = 0.5\text{GPa}$, $\sigma_Y = 20\text{MPa}$.

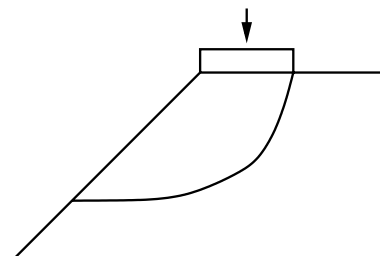


Figure 8 : Schematic representation of micromechanical law on a curved slipline

Figure 9 shows the undeformed and deformed meshes with the slipline contained in the shaded microstructural region. Limit analysis indicates that the shape of

the slipline could be either a logarithmic spiral (which is roughly the shape obtained in Figure 9) or a circle [Lubliner(1990)]. The sharply resolved deformation is again evident as is the rotation of the block and material beneath it.

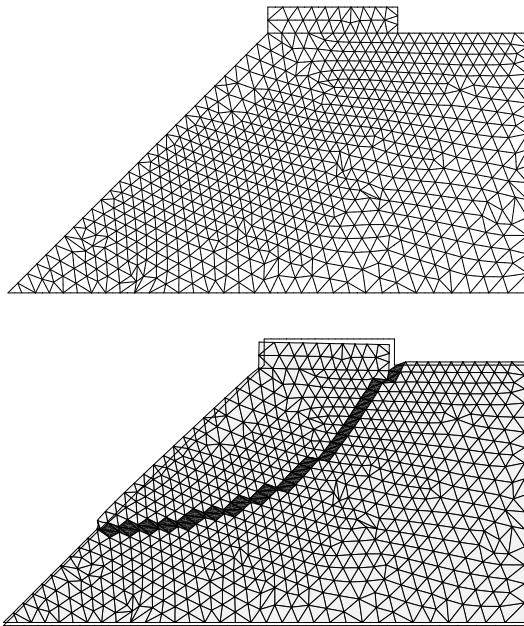


Figure 9 : Deformed mesh and shaded microstructural region for the wedge problem.

These numerical examples demonstrate the effectiveness of the variational multiscale approach at embedding micromechanical surface laws specified on sliplines and failure surfaces. The characteristics of the micromechanical laws such as softening response and well-defined thermodynamic dissipation are also retained.

Remark 3: While the three cases considered in this section are all shear-driven, unpublished calculations have been carried out for boundary value problems with mixed-mode evolution of traction on the surface Γ . On a similar note, in an experiment, a tension-loaded problem might fail due to ductile void growth; however, in this work the micromechanical surface law of Section 2 was deliberately chosen to represent the “failure” mechanism. Indeed, tension specimens often fail under shear band formation, which is modelled by the micromechanical surface law evolving in pure mode 2.

Remark 4: The meshes chosen for the three problems have not been refined around the micromechanical surface. Indeed, it is impossible to resolve the mesh down to what is essentially a lower-dimensional manifold. On the contrary, the point is that the *macroscopic* response obtained is physically correct when the present approach is used to embed micromechanical laws. The deformation of the mesh around the surface is restricted to a band of elements that contain the surface in each case. The observed deformations correspond to the coarse scale ones, $\bar{\mathbf{u}}$. The fine scale deformations, \mathbf{u}' have been projected on to the coarse scale and thus eliminated from the problem. This process results in embedding the micromechanical law in the macromechanical formulation.

4 Conclusion

The purpose of this communication is to demonstrate that the variational multiscale method can be used to embed micromechanics in the macromechanical formulation. The choice of surface laws for the micromechanical description was motivated by their simple form and relevance to problems involving localized deformation. The methods presented here are related to the strong discontinuities approach [Armero and Garikipati(1996); Armero and Callari(1999); Regueiro and Borja (1999); Borja and Regueiro(2001)] for strain localization problems. The difference lies in the fact that the present variational multiscale approach can be used to embed any specified surface law. In contrast, the strong discontinuities approach applies a distributional analysis on inelastic models admitting discontinuous solutions, to derive certain classes of surface laws. In the formulations involving discontinuous solutions, the form of the traction-displacement law is thus dependent upon the chosen inelastic material model. In the present paper, no such correspondence is necessary and a micromechanical model can be specified independently of the macromechanics. Work currently under progress will make the extension to micromechanical models applicable over small but finite-sized material subdomains. For instance, it may be of interest to incorporate material behavior at micron and submicron length scales around atomically sharp crack tips, micron-sized shear bands, voids and asperities. While

there exist micromechanical continuum theories² [Steinmann(1996; Fleck and Hutchinson(1997); Huang, Gao, Nix and Hutchinson(2000); Gurtin(2000)] that represent such fine scale physics, they are almost always applied to boundary value problems at micron length scales. Attempts to incorporate such theories in large scale structural calculations are confronted with issues of computational efficiency, complexity and robustness (the last two, due to the higher-order nature of the micromechanical theories). The ideas presented here can be extended to embed some of these theories in the classical macromechanical formulation, so that the fine scale physics is retained without sacrificing computational efficiency and robustness.

References

- Armero F. and Callari C.** (1999): Analysis of strong discontinuities in a saturated poro-plastic solid, *Int. J. Numer. Methods Engrg.*, Vol. 46, pp 1673-1698.
- Armero F. and Garikipati K.** (1995): Recent advances in the analysis and numerical simulation of strain localization in inelastic solids, *Proceedings of Computational Plasticity IV*, pp 547-561.
- Armero F. and Garikipati K.** (1996): An analysis of strong discontinuities in multiplicative finite strain plasticity and their relation with the numerical simulation of strain localization in solids, *Int. J. Solids and Structures*, Vol. 33, pp 2863-2885.
- Bazant Z.P.** (1976): Instability, ductility and size effect in strain softening concrete, *Journal of Engineering Mechanics*, Vol. 102, pp 331-344.
- Borja R.I. and Regueiro R.A.** (2001): Strain localization in frictional materials exhibiting displacement jumps, *Comp. Methods in Applied Mech. Engrg.*, Vol. 190, 2555-2580.
- Fish J. and Belsky V.** (1995): Multigrid method for periodic heterogeneous media part 1: convergence studies for one-dimensional case, *Comp. Methods in Applied Mech. Engrg.*, Vol. 126, pp 1-16.
- Fish J. and Belsky V.** (1995): Multigrid method for periodic heterogeneous media part 2: convergence studies for one-dimensional case, *Comp. Methods in Applied Mech. Engrg.*, Vol. 126, pp 17-38.
- Fleck N.A. and Hutchinson J.W.** (1997): Strain gradient plasticity, *Advances in Applied Mechanics*, Vol. 33, pp 295-361.
- Gao H., Huang Y., Nix W.D. and Hutchinson J.W.** (1999): Mechanism based strain gradient plasticity-I. Theory, *Journal of the Mechanics and Physics of Solids*, Vol. 47, pp 1239-1263.
- Garikipati K. and Hughes T.J.R.** (1998): A study of strain localization in a multiple scale framework – the one dimensional problem, *Comp. Methods in Applied Mech. Engrg.*, Vol. 159, pp 193-222.
- Garikipati K. and Hughes T.J.R.** (2000a): A variational multiscale approach to strain localization – formulation for multidimensional problems, *Comp. Methods in Applied Mech. Engrg.*, Vol. 188, pp 39-60.
- Garikipati K. and Hughes T.J.R.** (2000b): Embedding micromechanical laws in the continuum formulation – a multiscale approach applied to discontinuous solutions, *International Journal for Computational Civil and Structural Engineering*.
- Gurtin M.E.** (2000): On the plasticity of single crystals: free energy, microforces, plastic-strain gradients, *Journal of the Mechanics and Physics of Solids*, Vol. 48, pp 989-1036
- Huang Y., Gao H., Nix W.D., and Hutchinson J.W.** (2000): Mechanism-based strain gradient plasticity-II. Analysis, *Journal of the Mechanics and Physics of Solids*, Vol. 48, pp 99-128.
- Larsson R., Runesson K., and Akesson M.** (1995): Embedded localization band based on regularized strong discontinuity, *Proceedings of Computational Plasticity IV*, pp 599-609.
- Lubliner J.** (1990): *Plasticity Theory*, Macmillan Publishing Co.
- Moes N., Oden J.T., Kumar V. and Remacle J.** (1999): Simplified methods and a posteriori error estimation for the homogenization of representative volume elements (RVE), *Comp. Methods in Applied Mech. Engrg.*, Vol. 176, pp 265-278.
- Oden J.T., Kumar V. and Moes N.** (1999): Hierarchical modeling in heterogeneous solids, *Comp. Methods in Applied Mech. Engrg.*, Vol. 172, pp 3-25
- Oden J.T. and Pires E.B.** (1983): Nonlocal and non-

²The term “micromechanics” is used here to refer to any theory that describes material response at length scales of a micron and below. This would include strain gradient theories that resolve such micron-scale response, as well as those based upon defects and microstructure, such as the theory of dislocations.

linear friction laws and variational principles for contact problems in elasticity, *J. Applied Mechanics*, Vol. 50, pp 67-76.

Oden J.T. and Zohdi T.I. (1997): Analysis and adaptive modeling of highly heterogeneous elastic structures, *Comp. Methods in Applied Mech. Engrg.*, Vol. 148, pp 367-391.

Oliver J. (1996): Modeling strong discontinuities in solid mechanics via strain softening constructive equations. Part 1, *Int. J. Numerical Method Engrg.*, Vol. 39, pp 3375-3600.

Ottosen N.S. and Runesson K. (1991): Properties of discontinuous bifurcation solutions in elasto-plasticity, *Int. J. Solids and Structures*, Vol. 27, pp 401-421

Regueiro R. and Borja R. (1999): Finite element model of localized deformation in frictional materials taking a strong discontinuity approach, *Finite Elements in Analysis and Design*, Vol. 33, pp 283-315.

Rice J.R. (1976): The localization of plastic deformation, *Theoretical and Applied Mechanics*, pp 207-220.

Simo J.C., and Oliver J. (1994): A new approach to the analysis and simulation of strain softening in solids, *Fracture and Damage in Quasibrittle Structures*.

Simo J.C., Oliver J., and Armero F. (1993): An analysis of strong discontinuities induced by softening solutions in rate-independent solids, *Journal of Computational Mechanics*, Vol. 12, pp. 277-296.

Simo J.C., Taylor R.L. and Pister K.S. (1985): Variational and projection methods for the volume constraint in finite deformation elasto-plasticity, *Comp. Methods in Applied Mech. Engrg.*, Vol. 51, pp 177-208.

Steinmann P. (1996): Views on multiplicative elasto-plasticity and the continuum theory of dislocations, *Int. J. Engrg. Science*, Vol. 34, pp 1717-1735.

Svedberg T. and Runesson K. (1998): An algorithm for gradient-regularized plasticity coupled to damage based on a dual mixed FE-formulation, *Comp. Methods in Applied Mech. Engrg.*, Vol 161, pp 49-65.

William K. (1984): Experimental and computational aspects of concrete fracture, *Proc. Int. Conf. Comp. Aided Anal. and Design of Concrete Structures*, pp 33-70.

Zohdi T.I., Oden J.T. and Rodin G.J. (1996): Hierarchical modeling of heterogeneous bodies, *Comp. Methods in Applied Mech. Engrg.*, Vol. 138, pp 273-298.